LBL-37819
UC-414
CONF-9506279--5

# Lawrence Berkeley Laboratory
UNIVERSITY OF CALIFORNIA

## Accelerator & Fusion Research Division

Presented at the International Workshop on Collective Effects and Impedance for B-Factories, KEK, Tsukuba, Japan, June 12–17, 1995, and to be published in the Proceedings

RECEIVED
JAN 2 4 1996
OSTI

**Observation of Collective Effects at the Advanced Light Source**

J.M. Byrd, W. Barry, J.N. Corlett, J. Fox, D. Teytelman

October 1995

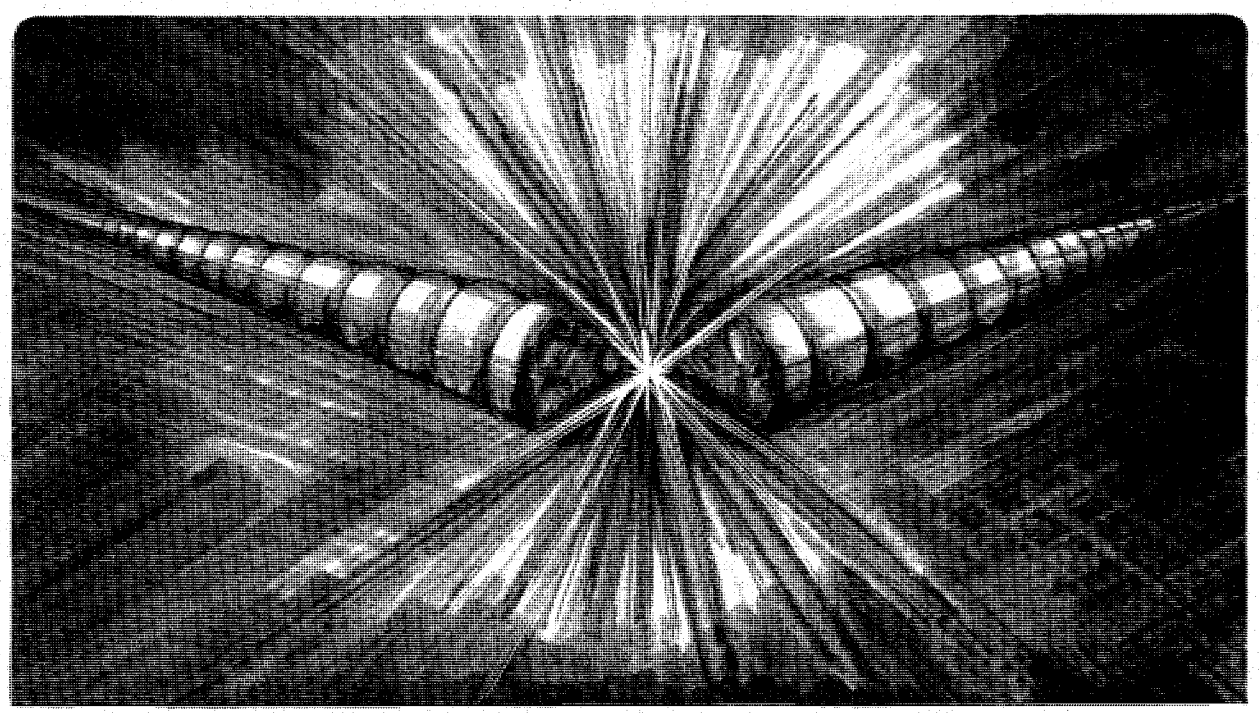

**Prepared for the U.S. Department of Energy under Contract Number DE-AC03-76SF00098**

**DISCLAIMER**

This document was prepared as an account of work sponsored by the United States Government. While this document is believed to contain correct information, neither the United States Government nor any agency thereof, nor The Regents of the University of California, nor any of their employees, makes any warranty, express or implied, or assumes any legal responsibility for the accuracy, completeness, or usefulness of any information, apparatus, product, or process disclosed, or represents that its use would not infringe privately owned rights. Reference herein to any specific commercial product, process, or service by its trade name, trademark, manufacturer, or otherwise, does not necessarily constitute or imply its endorsement, recommendation, or favoring by the United States Government or any agency thereof, or The Regents of the University of California. The views and opinions of authors expressed herein do not necessarily state or reflect those of the United States Government or any agency thereof, or The Regents of the University of California.

Ernest Orlando Lawrence Berkeley National Laboratory
is an equal opportunity employer.

DISCLAIMER

Portions of this document may be illegible in electronic image products. Images are produced from the best available original document.

LBL-37819
CBP Note-159

# Observations of Collective Effects at the Advanced Light Source*

J. M. Byrd, W. Barry, J.N. Corlett, J. Fox, D. Teytelman

Lawrence Berkeley National Laboratory
University of California
Berkeley, California 94720

Submitted to the Proceedings of the International Workshop on Collective Effects and Impedance for B-factories, KEK, Tsukuba, Japan, June 12-17, 1995

* This work was supported by the Director, Office of Energy Research, Office of Basic Energy Sciences, Materials Sciences Division, of the U. S. Department of Energy, under Contract No. DE-AC03-76SF00098.

MASTER
DISTRIBUTION OF THIS DOCUMENT IS UNLIMITED

# Observations of collective effects at the Advanced Light Source*†

J. M. Byrd, W. Barry, J. N. Corlett
*Lawrence Berkeley Laboratory, One Cyclotron Road, Berkeley, California 94720 USA*

J. Fox, D. Teytelman
*Stanford Linear Accelerator Center, Stanford University, Stanford, California 94309 USA*

We present a summary of measurements of single beam collective effects in the Advanced Light Source (ALS). We describe measurements of coupled–bunch instabilities, including some recent results using the newly commissioned feedback systems and the results of an initial search for the fast ion instability. Single bunch effects include bunch lengthening, energy spread increase, HOM loss measurements, head-tail damping rates, current dependent tune shifts, and transverse mode coupling instability threshold. The longitudinal measurements are consistent with a broadband impedance $|Z_\parallel/n|_{eff} = 0.22 \pm 0.07\ \Omega$ and transverse measurements indicate broadband impedances of $Z_{y,eff} = 155\ k\Omega/m$ and $Z_{x,eff} = 58\ k\Omega/m$.

## I. INTRODUCTION

Collective effects are expected to be one of the main challenges in operating a successful B–Factory. Third generation light sources are already struggling and meeting some of the challenges of collective effects, particularly multibunch instabilities. At the Advanced Light Source (ALS) in Berkeley, we observe many of the collective effects which will be important in a B–Factory. This paper presents a summary of observations and measurements of single and multibunch collective effects at the ALS to date.

The ALS is a 1.0–1.9 GeV electron storage ring optimized for producing high brightness synchrotron radiation. General parameters are given in Table I. In the original design of the ALS, the intention was to keep the current per bunch relatively low but have as many bunches as possible in order to avoid single bunch collective effects. The resulting multibunch collective effects (i.e. instabilities) could be cured by use of feedback systems. For the most part, this has been the case. Machine performance since the original commissioning in March 1993 has been dominated by longitudinal coupled–bunch instabilities and single bunch effects have been negligible for most conditions. Feedback systems have recently been commissioned which damp longitudinal and transverse coherent dipole oscillations.

The first two sections of this paper describe observations of multibunch effects in the longitudinal and transverse directions, including the results of a brief initial study to search for the fast ion instability. A short discussion of the causes of saturation of CB oscillations is also given. The last section presents a summary of the single bunch measurements. Several of the measurements, calculations, and numerical simulations are described in more detail in earlier papers [1–4].

## II. COUPLED–BUNCH INSTABILITIES

Multibunch collective effects arise from wakefields which persist until passage of the following bunch. Coupled–bunch (CB) oscillations in the longitudinal direction are expected to be driven by high–$Q$ monopole higher–order modes (HOMs) of the two RF cavities and in the transverse directions the dipole HOMs and the resistive wall impedance. Measurements and calculations of the driving impedances are described elsewhere [5]. Beam loading of the fundamental mode is relatively small and causes no problems for operation.

---

*This work was supported by the Director, Office of Energy Research, Office of Basic Energy Sciences, Materials Sciences Division, of the U.S. Department of Energy under Contract No. DE-AC03-76SF00098.
†presented at the Workshop on Collective Effects in B–Factories, KEK, June 1995.

| Parameter | Description | Value |
|---|---|---|
| $E$ | Beam energy | 1.5 GeV |
| $C$ | Circumference | 196.8 m |
| $f_{rf}$ | RF Freq. | 500 MHz |
| $\sigma_\epsilon$ | RMS $\delta E/E$ | 7.1e-4 |
| $h$ | Harmonic Number | 328 |
| $I_0$ | Design beam current | 0.4 A |
| $I_b$ | Bunch current | 1–2 mA |
| $\alpha$ | Momentum compaction | 1.594e-3 |
| $Q_s$ | Synchrotron tune | 0.006 |
| $\sigma_\ell$ | RMS natural bunch length | 5-10 mm |
| $\tau_{rad}$ | Longitudinal damping time | 13.5 msec |
| $\tau_{rad,x,y}$ | x,y damping times | 15.3,21.5 msec |
| $Q_{x,y}$ | Betatron tunes (x,y) | 14.28, 8.18 |

TABLE I. Nominal ALS storage ring parameters.

### A. Longitudinal

During normal operation the storage ring filling pattern has every RF bucket filled roughly equally with a ~2.5% gap nominally for ion clearing to a total current of ~400 mA. Spontaneous longitudinal oscillations occur at 5-30 mA total beam current without much dependence on the fill pattern but with a dependence on cavity temperatures. Beam oscillations saturate at a level which slowly increases with current. Oscillation amplitudes have been measured at 5–10$\sigma_\ell$. The oscillations do not appear to cause any beam loss but rather improve the lifetime, probably from the dilution of the beam density. However, the energy oscillations cause broadening of the undulator harmonics, reducing the effective brightness from the insertion devices.

The first part of this section describes the results of studies of the longitudinal instabilities prior to the recent operation of the longitudinal feedback (LFB) system. This is followed by some brief comments on operation of the LFB and measurements of growth rates made using it.

We diagnosed the instabilities by passively observing the beam spectrum using a BPM sum signal. In order to simplify identification of the coupled oscillation modes and correlate them with the driving impedance, we used fill patterns of equally spaced, equally charged bunches. The exponential growth rate of CB mode $\ell$ is given by [7]

$$\frac{1}{\tau} = \frac{1}{2} f_0 \frac{I_0 h \alpha}{(E/e) Q_s} Re\left[Z_\parallel\right]^\ell_{eff} \tag{1}$$

where

$$\left[Z_\parallel\right]^\ell_{eff} = \sum_{p=-\infty}^{p=+\infty} \frac{\omega_p}{\omega_{rf}} e^{-(\omega_p \sigma_\tau)^2} Z_\parallel(\omega_p) \tag{2}$$

and

$$\omega_p = (pN + \ell + Q_s)\omega_0. \tag{3}$$

The effective impedance, $\left[Z_\parallel\right]_{eff}$, represents the sum of the RF cavity resonant mode impedance weighted by the single bunch spectrum. The condition for a beam instability occurs when the growth rate given in Eq. 1 exceeds the sum of the natural damping mechanisms such as radiation damping and Landau damping. All beam measurements were restricted to symmetric fill patterns because of the relative simplicity of the normal modes.

Observed on a spectrum analyzer, the beam current spectrum has frequency components at multiples of the bunch harmonic frequency, $Nf_0$, and the oscillations of individual CB modes appear as phase modulation (PM) sidebands about the bunch harmonics. The amplitude of phase modulation of CB mode $\ell$ can be determined from the ratio of the first order sideband to the carrier. Note that all $N$ CB modes can be measured in a frequency span of $pNf_0$ to $pNf_0 + \frac{Nf_0}{2}$.

Expressed formally, for a symmetric fill pattern of $N$ bunches, the signal from an ideal pickup is a series of delta function impulses given by [6]

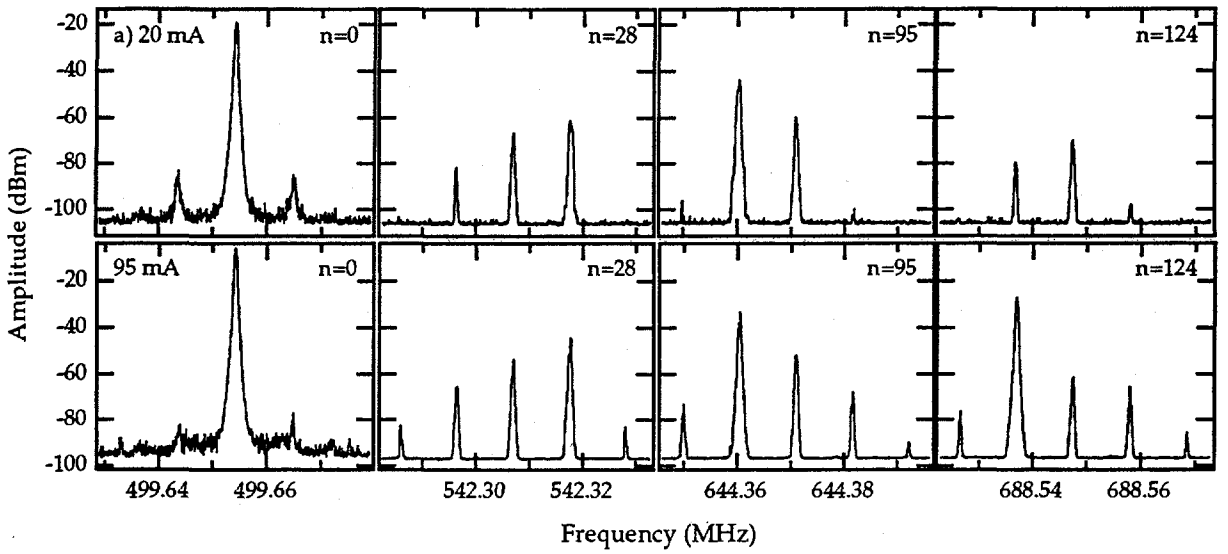


FIG. 1. Raw frequency spectra near selected revolution harmonics. The number of revolution harmonics (n) from the RF frequency is indicated in each plot. The top row is measured at 20 mA and the bottom at 95 mA of total beam current.

$$s(t) = 2k_{pu}q \sum_{n=-\infty}^{\infty} \sum_{m=1}^{N} \delta(t - nT_0 - m\frac{T_0}{N} - \tau_m \cos(\omega_s t + \phi_m)) \tag{4}$$

where $q$ is the bunch charge, $k_{pu}$ is the loss parameter of the pickup, $\tau_m$ the oscillation amplitude of bunch $m$ in units of time, $\omega_s$ the angular synchrotron frequency, and $\phi_m$ the relative phase of oscillation of bunch $m$. The summations are over bunch number $m$ and turn number $n$. The pickup signal in the frequency domain can be expressed as

$$s(\omega) = 2k_{pu}q \sum_{l=0}^{N-1} \sum_{k=-\infty}^{\infty} (-j)^k J_k(\omega\tau_l) \sum_{p=-\infty}^{\infty} \delta(\omega - pN\omega_0 - k(l + Q_s)\omega_0) \tag{5}$$

where $\tau_\ell$ is the oscillation amplitude of CB mode $\ell$ in units of time, and $J_k$ is the $k$th order Bessel function. From this, the amplitude of any CB mode can be found from the ratio of the sideband to carrier amplitude. At the frequencies used in the measurements, the bunch can be considered a point charge.

In our measurements, the storage ring was filled in symmetric patterns of 82 and 328 bunches and the amplitudes of all longitudinal CB modes were measured as a function of current. Unavoidable variations in the charge of each bunch led to small frequency components at revolution harmonics between bunch harmonics and were used as a measure of the uniformity of the fill pattern. We observed 1–5% variations in the bunch uniformity around the ring. The process of recording the sidebands of many revolution harmonics was automated by way of a MacIntosh computer equipped with a GPIB interface.

Shown in Figure 1 are some representative beam spectra measured at 20 and 95 mA showing the CB mode oscillations which appear as upper or lower sidebands of the revolution harmonics. The center peak in each spectrum is the residual revolution harmonic arising from the asymmetry in the bunch charges. The sidebands at $f_s$ and $2f_s$ are first and second order PM sidebands and are not related to internal bunch modes. The amplitude of all CB modes for the 328 bunch configuration is shown in Figure 2. The oscillation amplitudes are expressed in degrees of phase modulation at the RF frequency, 500 MHz.

The patterns observed in the amplitude of the CB modes can be interpreted by comparing them with the effective impedance, for a given bunch filling pattern evaluated using the measured parameters of the RF cavity HOMs. The real part of $[Z_\parallel]_{eff}$ for the 328 bunch case is shown in Figure 2c. The left axis is the effective impedance and the right axis the corresponding growth rate at 20 mA. The dotted line represents the effective impedance resulting in growth for CB modes corresponding to upper sidebands in the frequency range. The dashed line is the effective impedance resulting in growth for lower sidebands in the same frequency range. The aliased HOM's are labeled according to their resonant frequency.

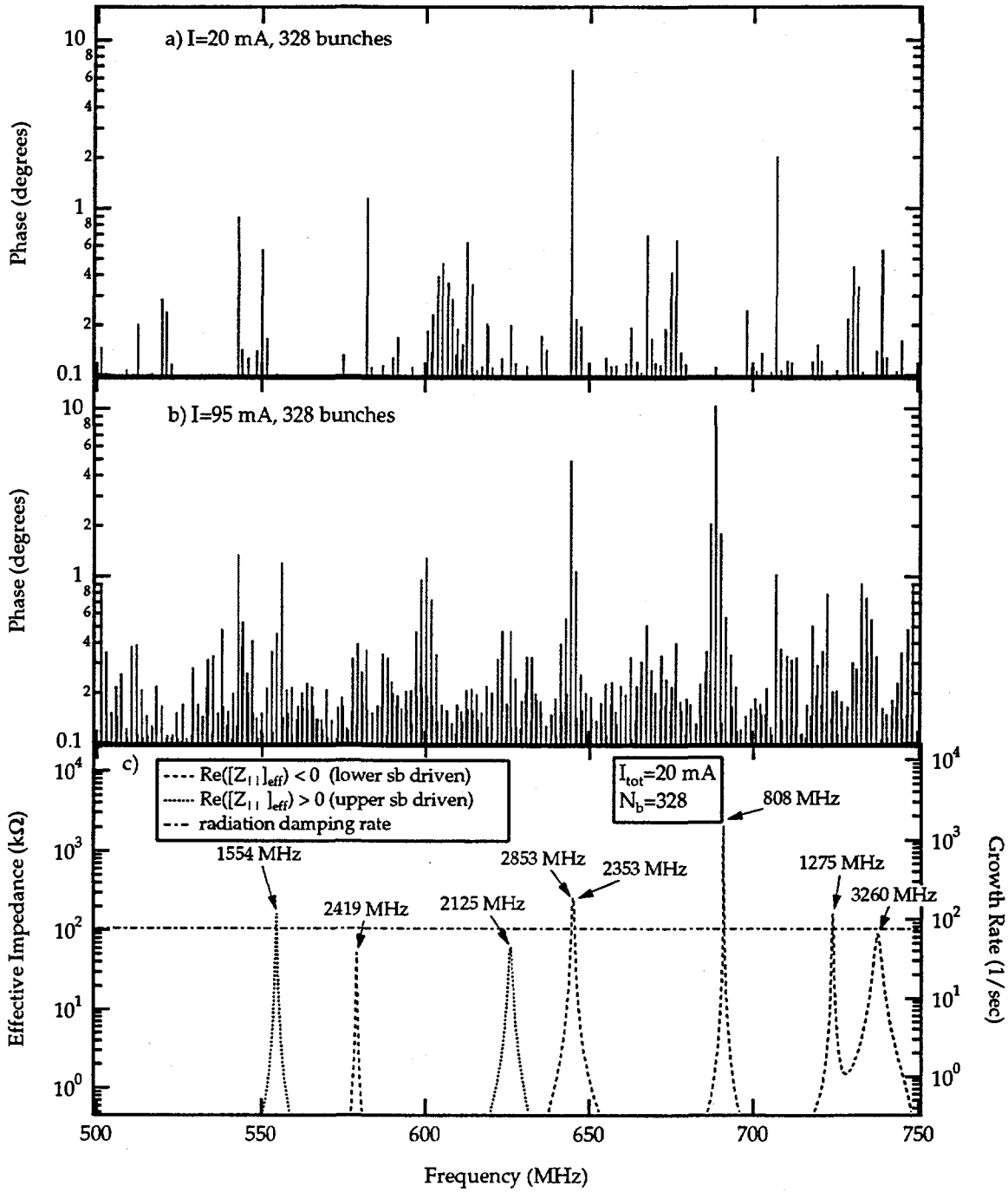


FIG. 2. a-b) Measured spectrum of first-order longitudinal sidebands for 328 bunches in the frequency range 500-750 MHz for 20 and 95 mA. c) Real part of the RF cavity impedance aliased into the same frequency range. The corresponding growth rate for 20 mA is shown on the right axis.

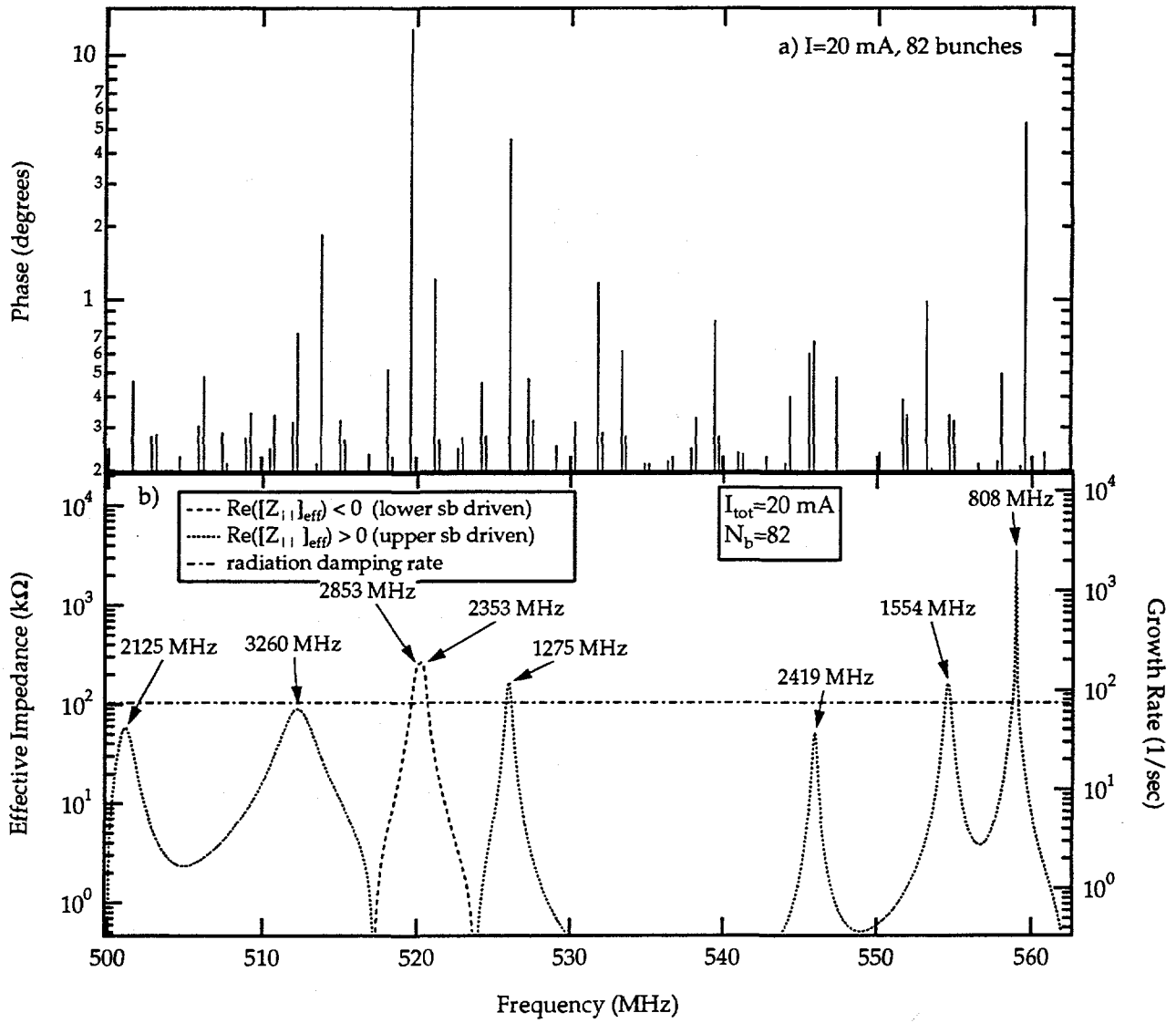


FIG. 3. a) Measured spectrum of first-order longitudinal sidebands for 82 bunches in the frequency range 500-625 MHz for 20 mA. b) Real part of the RF cavity impedance aliased into the same frequency range. The corresponding growth rate for 20 mA is shown on the right axis.

Comparing the effective impedance with the CB mode amplitudes for each filling pattern, we can correlate the beam spectrum with the measured impedance and positively identify the driving HOMs. At 95 mA, the strongest CB modes are driven by the high-$Q$ TM-011 HOM ($f_r$=808 MHz) and the next strongest CB modes by the HOMs at 2.3 and 2.8 GHz. Experiments changing the cavity temperature and tuner position show that the stability of the CB mode driven by the high-$Q$ HOM changes greatly with cavity conditions. Cavity conditions do not greatly affect the lower-$Q$ HOMs. We see a similar correlation with the effective impedance in the 82 bunch case as shown in Figure 3.

Individual modes grow in amplitude as a function of beam current, limiting at a phase excursion of approximately 10 degrees at 500 MHz. As the current increases, other modes grow in amplitude until many modes are present at approximately the same amplitude. At a current of 400 mA, the amplitude of coherent oscillation appears to decrease. Preliminary measurements using a streak camera indicate that at lower total currents (< 100 mA) the bunch oscillations remain coherent. At higher currents, we observe turbulent motion within the bunch which effectively lengthens the bunch and increases the energy spread. This probably results from a combination of the growth of the centroid motion from the instability and decoherence. Note that this effect is distinct from the microwave instability affecting single bunches.

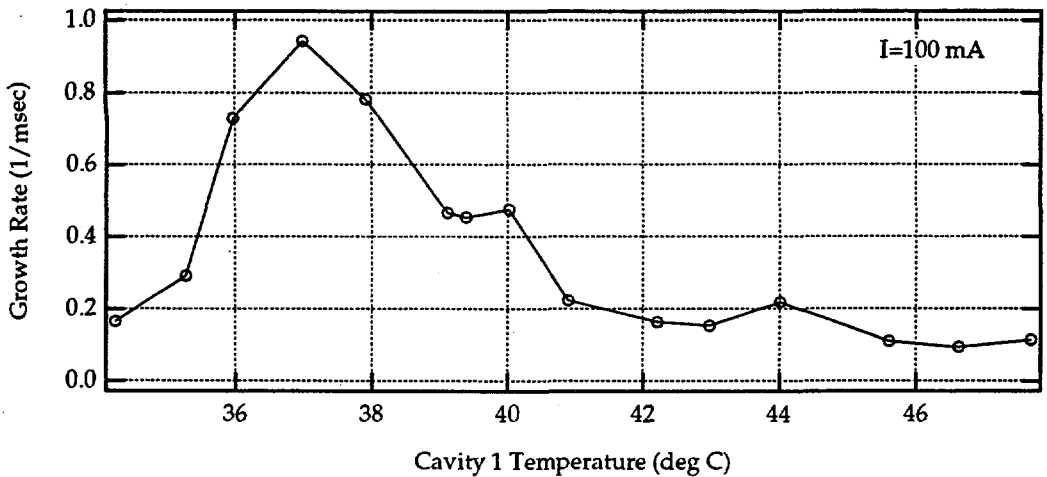


FIG. 4. Measured longitudinal growth rates vs. tuning of one of the RF cavities. Tuning of the HOMs can be controlled by varying the cavity cooling water temperature.

Recent operation of the longitudinal feedback system has allowed us to measure growth rates by turning the feedback off and then on. The LFB system itself is discussed elsewhere [8,9], including a contribution to these proceedings which includes more details on recent results. The digital feedback system records the oscillations of all bunches and subsequent processing yields the growth rates of the unstable CB modes. We have been able to map the growth rates vs. cavity temperature to determine the range of acceptable cavity tuning conditions. Shown in Figure 4 is a plot of the growth rate vs. the temperature of cooling water for one of the RF cavities at 100 mA total beam current. As discussed above, the fastest growth rate is very sensitive to the tuning of the high-$Q$ TM-011 mode ($f_r$=808 MHz) and somewhat less sensitive to the tuning of the HOMs at 2.3 and 2.8 GHz. Work is in progress to study the growth rates of the various CB modes vs. cavity tuning. This will clearly allow to distinguish the effects of tuning of the strongest HOMs.

### B. Transverse

Transverse CB oscillations have not been a problem because of the presence of large longitudinal oscillations. This is further discussed in the next section. However, with the successful operation of the longitudinal feedback system, transverse instabilities have become immediately apparent. Shown in Figure 5 is a plot of the unstable mode spectrum for vertical and horizontal motion. In each case, feedback systems were operational in the other two directions of motion. The calculated effective transverse impedance using the measured cavity dipole HOM parameters and the resistive wall impedance are shown below each mode spectrum for comparison. In the vertical case, the beam spectrum is dominated by the effect of the resistive wall impedance and one relatively high-$Q$ HOM, for which we have observed sensitivity to temperature and tuner conditions. In the horizontal case, the spectrum is dominated by several high-$Q$ HOMs at 808 and 1129 MHz. We observe strong sensitivity of the beam spectrum to tuning of both of these modes. It is this fact which presents the main operational difficulty in adjusting the feedback systems for maximum stability. It is difficult to find a tuning condition for both cavities which satisfies requirements for all three directions of motion.

Growth rates of unstable oscillations can be measured in several ways. We use a spectrum analyser in tuned receiver mode with the center frequency set to either a horizontal or vertical CB mode frequency and modulate the gain of the transverse FB, usually from fully on to fully off. An example of a measurement at a beam current of 350 mA is shown in Figure 6. In this case, the beam signal is a vertical difference signal. When the VFB is turned off the unstable mode begins to grow with a growth time of 1.1 msec and is damped with a characteristic time of 0.33 msec when the VFB is turned on again. This corresponds roughly to a FB gain of 1.5 kV/mm. The growth and damping rate can then be measured as a function of current, FB gain for all CB modes. We have just recently begun such measurements. We are also developing the beam transfer function method for measuring the growth rate and the effective impedance. This technique is also useful for diagnosing the transverse feedback system itself.

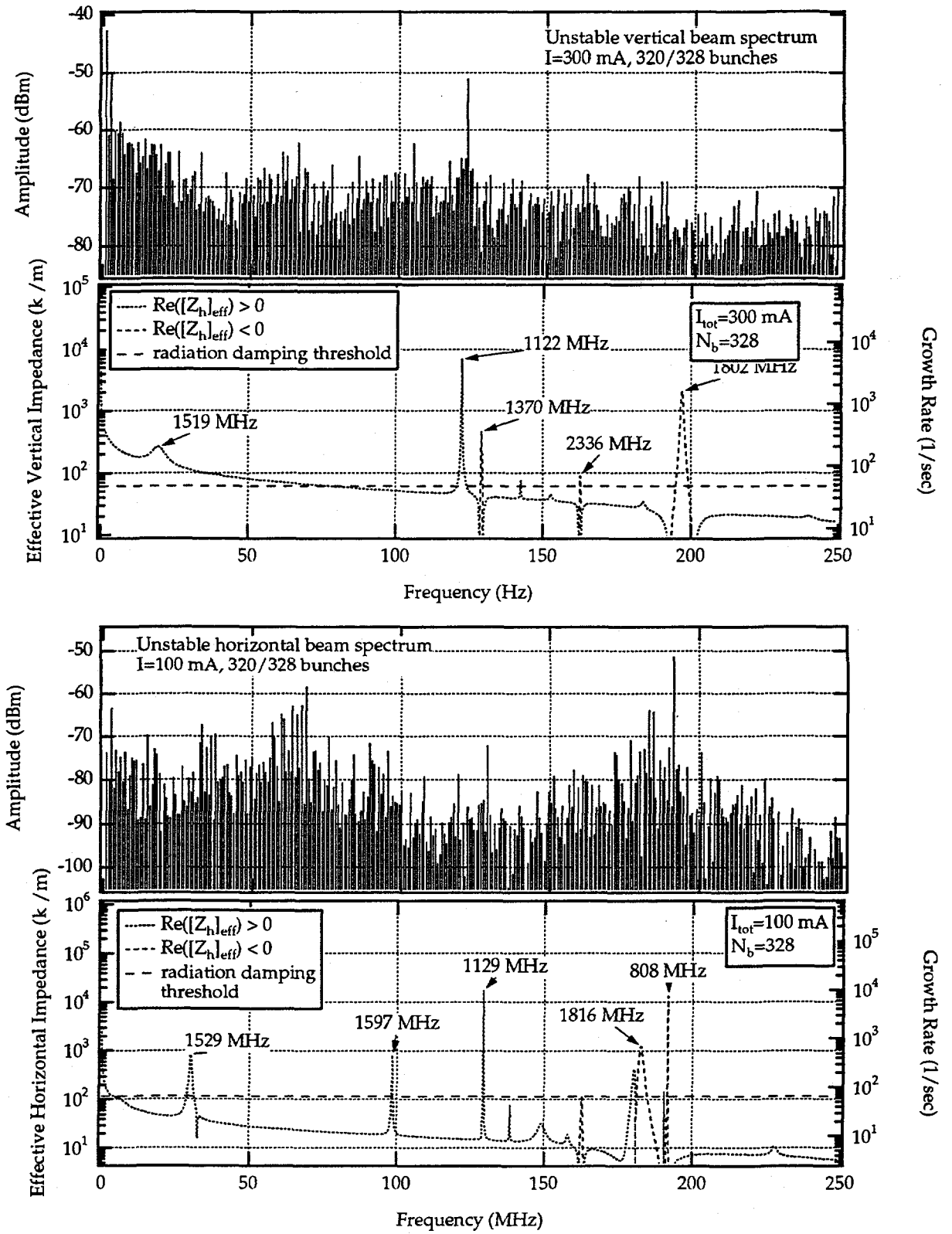


FIG. 5. Measured unstable vertical and horizontal CB mode spectrum. The calculated effective impedance using measured cavity dipole HOMs and resistive wall impedance is plotted below each mode spectrum for comparison.

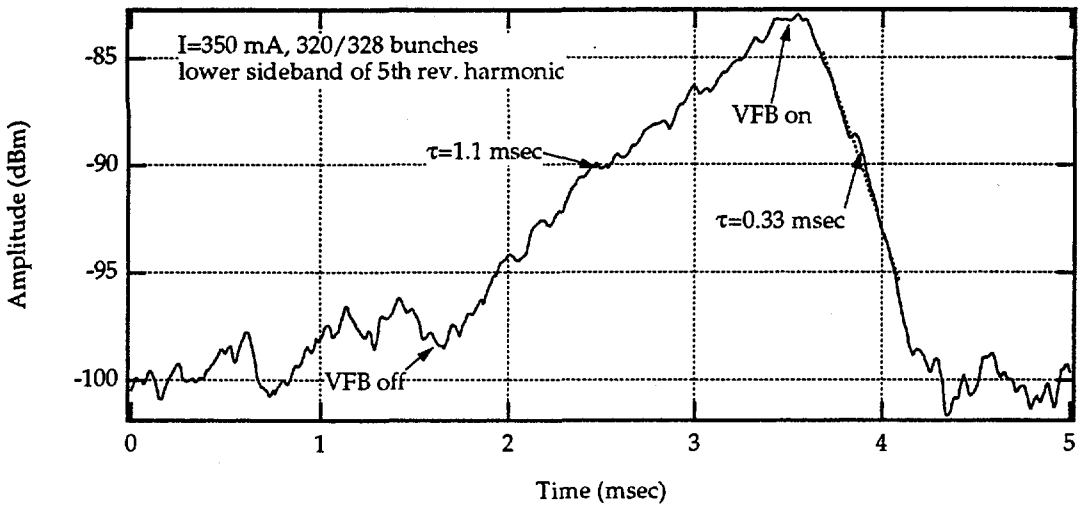


FIG. 6. Example of a CB growth and damping rate measurement using the spectrum analyzer in tuned receiver mode.

### C. Initial Search for the Fast–Ion Instability

A new instability mechanism resulting from the interaction of an electron beam and residual gas ions has been predicted by Raubenheimer and Zimmerman [12,13]. The instability is called the fast ion instability (FII) and has been calculated to be a potential limitation in the design of several future storage rings such as PEP-II HER, NLC Damping Ring, as well as several existing rings such as ALS and ESRF. This effect is distinguished from the familiar ion–trapping instability in that it arises from a single pass of the electron beam (i.e. bunch train) and thus is more like a linac–type instability and should be present even with an ion clearing gap. The instability is also predicted to saturate at relatively low amplitudes with the largest amplitude of about 1 $\sigma_y$ [14]. This section describes some beam measurements suggestive of ion effects and the results of an experiment to determine if the effects were from the FII.

The goal of this study was to determine whether any unusual beam oscillations exist beyond those generated by cavity HOMs. We used a simple BPM difference signal observed on a spectrum analyzer and also observed the transverse beam profile on a synchrotron light monitor. The initial observations were made in the nominal user configuration of the storage ring. Measured vacuum pressures were about $10^{-9}$ Torr.

During commissioning of the transverse CB feedback systems, we noticed residual vertical betatron sidebands with a pattern suggestive of ion effects with all feedback systems operational. The amplitudes of upper and lower sidebands at the first 20 revolution harmonics for three different currents are shown in Figure 7. The signals appear at first glance to be consistent with the resistive wall effect, except that the signals begin to decrease approaching low frequency. Furthermore the frequency of the peak signals increases with current. There were not any other significant residual sidebands over the 0–250 MHz span. We do not yet have a good calibration of the absolute amplitude of the beam oscillations but we believe that the oscillations are on the order of a micron. Furthermore, we could not qualitatively observe any oscillations on the transverse profile monitor.

Although the signals are not inconsistent with CB motion driven by a cavity HOM that changes frequency with current because of cavity detuning, we became suspicious of an ion effect because of the dependence of the frequency shift with current and because all other beam signals present without feedback were damped to the noise floor of the spectrum analyzer.

Consider the ion oscillation frequency in the beam's potential well is given by

$$f_{ion} = \frac{c}{2\pi}\left[\frac{4N_b r_p}{3L_{sep}\sigma_y(\sigma_x+\sigma_y)A}\right]^{1/2} \tag{6}$$

where $A$ is the atomic mass number of the ions, $N_b$ is the number of electrons/bunch, $L_{sep}$ the bunch spacing, $\sigma_x$ and $\sigma_y$ the horizontal and vertical beam sizes, and $r_p$ the classical proton radius ($\approx 1.5 \times 10^{-18}$ m.) Notable features are the increase in the ion frequency with the square root of the beam current, and decrease in the frequency with the vertical beam size. We expect the beam to oscillate at the ion frequency.

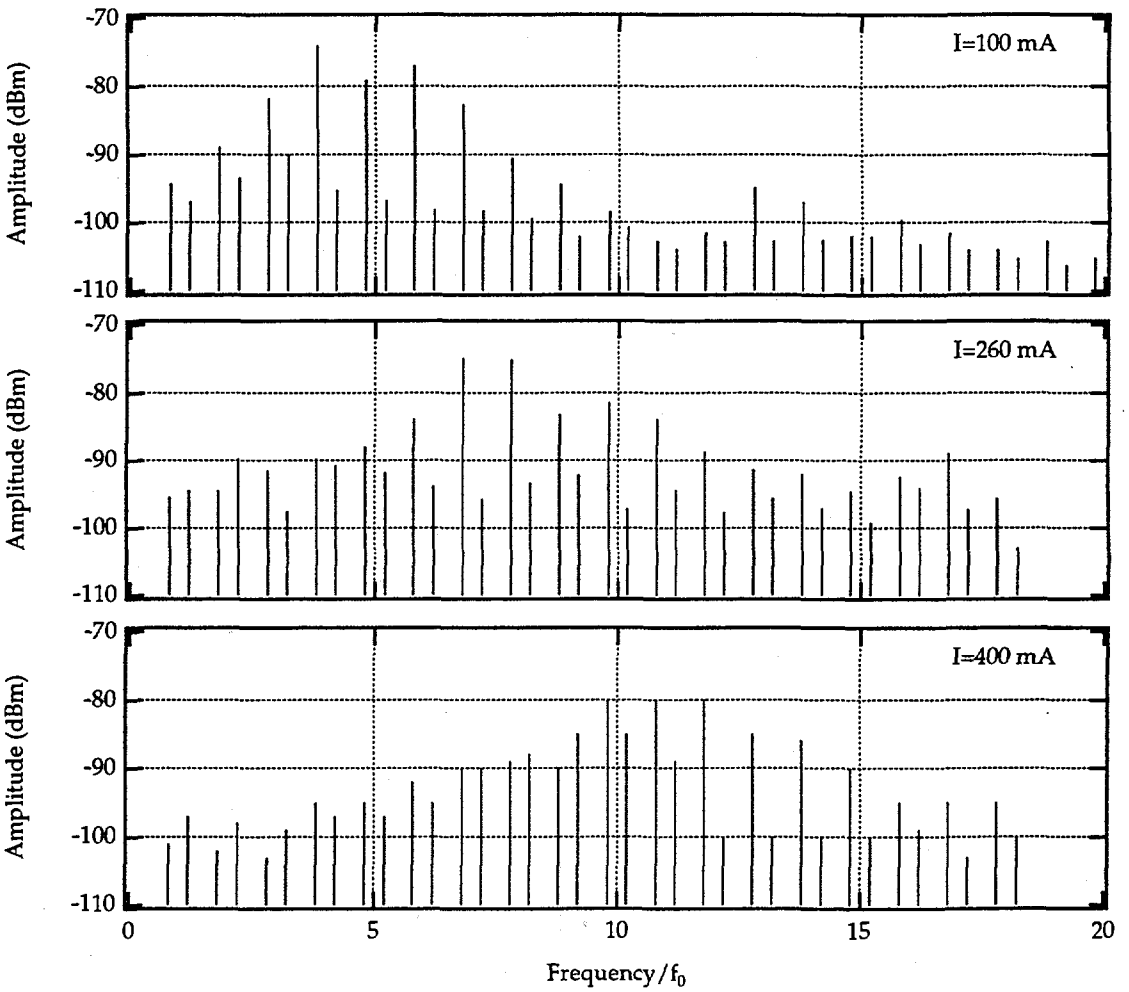


FIG. 7. Amplitudes of residual vertical betatron sidebands measured in the 320/328 fill pattern at 3 total beam currents.

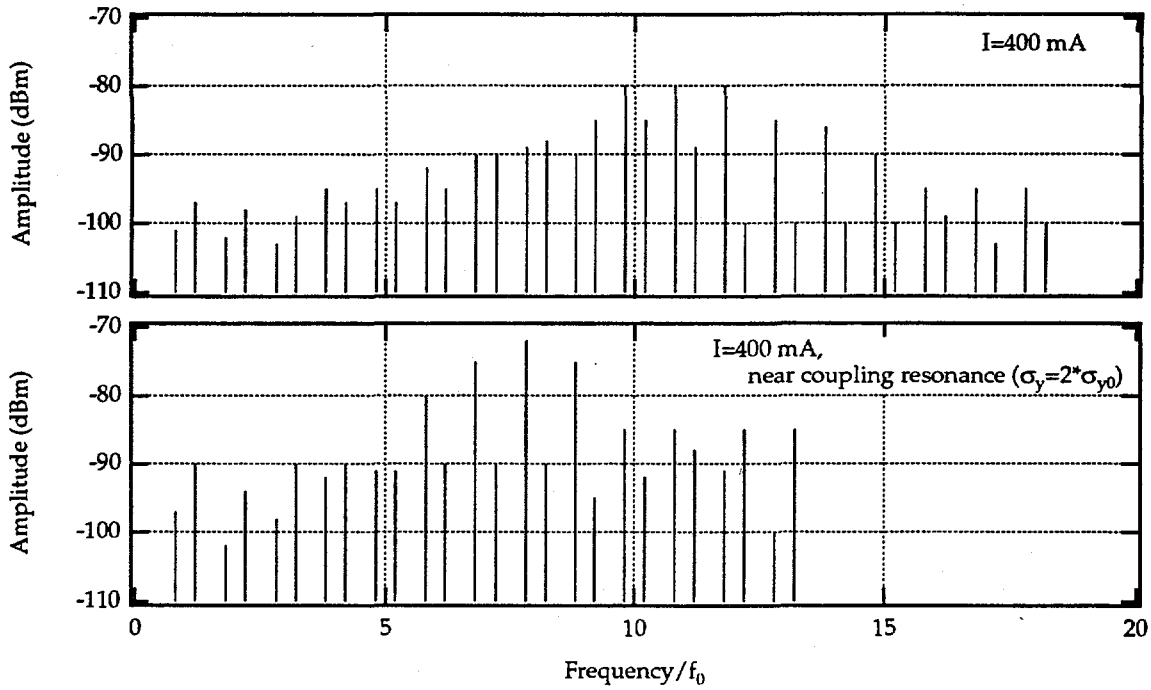


FIG. 8. Residual vertical betatron sidebands away and near the betatron coupling resonance.

Using approximate average beam sizes, $\sigma_{x,y}$ =101 and 17 $\mu$m, and assuming that the ion species is CO ($A$ =28), the calculated ion frequency at 400 mA is 17 in units of the revolution frequency (1.52 MHz). The peak frequency of the signals in Figure 7 increases approximately with the square root of the beam current. Furthermore, beam-ion interactions destabilize beam modes corresponding to lower sidebands. The absolute frequency of the peak is somewhat lower than expected but this could possibly be improved by using more accurate values for the vertical emittance which were not available at the time the measurement was made.

The effect of an increase in the vertical beam size is shown in Figure 8. An increase of about a factor of 2 causes a corresponding decrease in the peak frequency of the betatron signals. This effect is not consistent with motion driven by an HOM and suggests the presence of ions. The beam size was adjusted by running closer to the betatron coupling resonance.

Our experiment to check if the signals we observed resulted from the FII consisted simply of increasing the beam gap and observing whether the residual signals persisted. In summary, for gaps of 1/4 and 1/2 of the ring, the residual signals disappeared. Unfortunately, circumstances did not allow variation of the feedback system gain to check if the residual oscillations appeared at a lower feedback gain (the feedback damping time for the conditions during the experiment has been measured to be $\sim 50 - 100$ $\mu$sec.) Our conclusion from this experiment is that the FII is not present with a growth rate faster than the damping rate of the feedback system. We believe the signals in the 320/328 fill pattern to result from a benign form of beam–ion interaction, probably ion–trapping. This effect alone deserves more study.

Theoretical study of the FII is continuing at a rapid pace with the initial predicted growth rates decreasing from effects which were originally ignored such as nonlinearities, decoherence, and variations in the ion frequency around the ring. Plans for future studies at ALS include variation of feedback gain and a controlled variation of the vacuum pressure.

## III. COUPLED-BUNCH SATURATION

During our studies of coupled–bunch oscillations we were were puzzled by two effects: the limiting of longitudinal oscillations and the lack of significant transverse oscillations. This section presents some ideas, results of numerical simulations, and measurements aiding our understanding of these phenomena which emerged during this period. Understanding of these limiting mechanisms is not directly relevant to operation of a multibunch storage ring because in practice feedback systems are still required to damp the limited

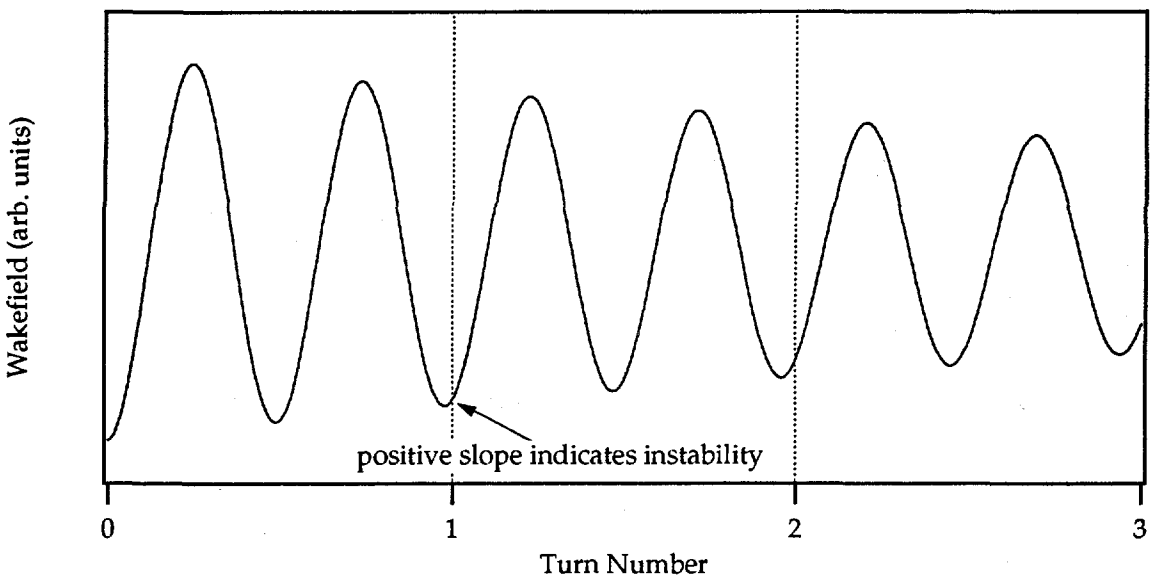


FIG. 9. Physical picture of saturation mechanism for a multiturn instability. Growth stops when the oscillations approach a half wavelength of the driving wakefield.

oscillations. However, it is perhaps of more than academic interest, especially if the limiting mechanisms can be controlled such that the oscillations saturate at a much lower level which is acceptable without the construction of expensive feedback systems.

### A. Longitudinal Saturation Mechanism

To illustrate the saturation mechanism, consider the simple model of a multi-turn instability shown in Figure 9. A bunch passes through a an RF cavity at turn 0 and excites the single cavity resonance, which then oscillates at its resonant frequency. The cavity frequency has been chosen to be very low for purposes of illustration. On the arrival at the next turn, the bunch sees either a positive, negative, or zero slope of its own wakefield. It is the sign of the slope which determines whether the oscillation is damped or growing. This is the well-known Robinson instability.

At the onset of the bunch's oscillation growth, the bunch is oscillating over a very small fraction of a period of the wakefield. As the oscillation amplitude becomes comparable to approximately a half period of the wakefield, it samples equally over positive and negative slopes and the resulting destabilizing effect averages to zero and the oscillations do not grow further. An equivalent mathematical description has been given for a single bunch multiturn instability by Krinsky [10] which holds that, to first order, the oscillation limits when the amplitude of phase oscillation at the frequency of the HOM is at the first zero of the zeroth order Bessel function, $J_0$. Other saturation mechanisms [11] involving nonlinear Landau damping may be related to the above mechanism and may explain some of the turbulent behavior observed in beam measurements and in simulations. However, this subject is beyond the scope of this paper.

In order to further study the saturation effect for many bunches and many HOMs under a variety of conditions, a simple numerical tracking code was developed. Each bunch is treated as a macroparticle and HOMs are all modeled as resonators. More details on the simulation are given elsewhere [3].

Shown in Figure 10 is the result of a simulation with symmetric fill pattern of 4 bunches under nominal ALS conditions. Only one resonator HOM is used and is purposely tuned to the frequency of an unstable CB mode at approximately 4 times the RF frequency. A high–$Q$ HOM is used so that only one CB mode is affected. Figure 10a shows the phase oscillations initially grow with the calculated growth rate until the growth appears to saturate at the expected amplitude. The complex behavior of the phase oscillations subsequent to the initial saturation is not yet understood but is believed to result from the combination of the nonlinearity of wakefield and the the RF voltage. Figure 10b shows the inverse relationship between the initial saturation amplitude and the HOM frequency. Simulations using the HOMs of the ALS cavities shows similar saturation behavior which qualitatively agrees with measurements of the amplitude of beam oscillations.

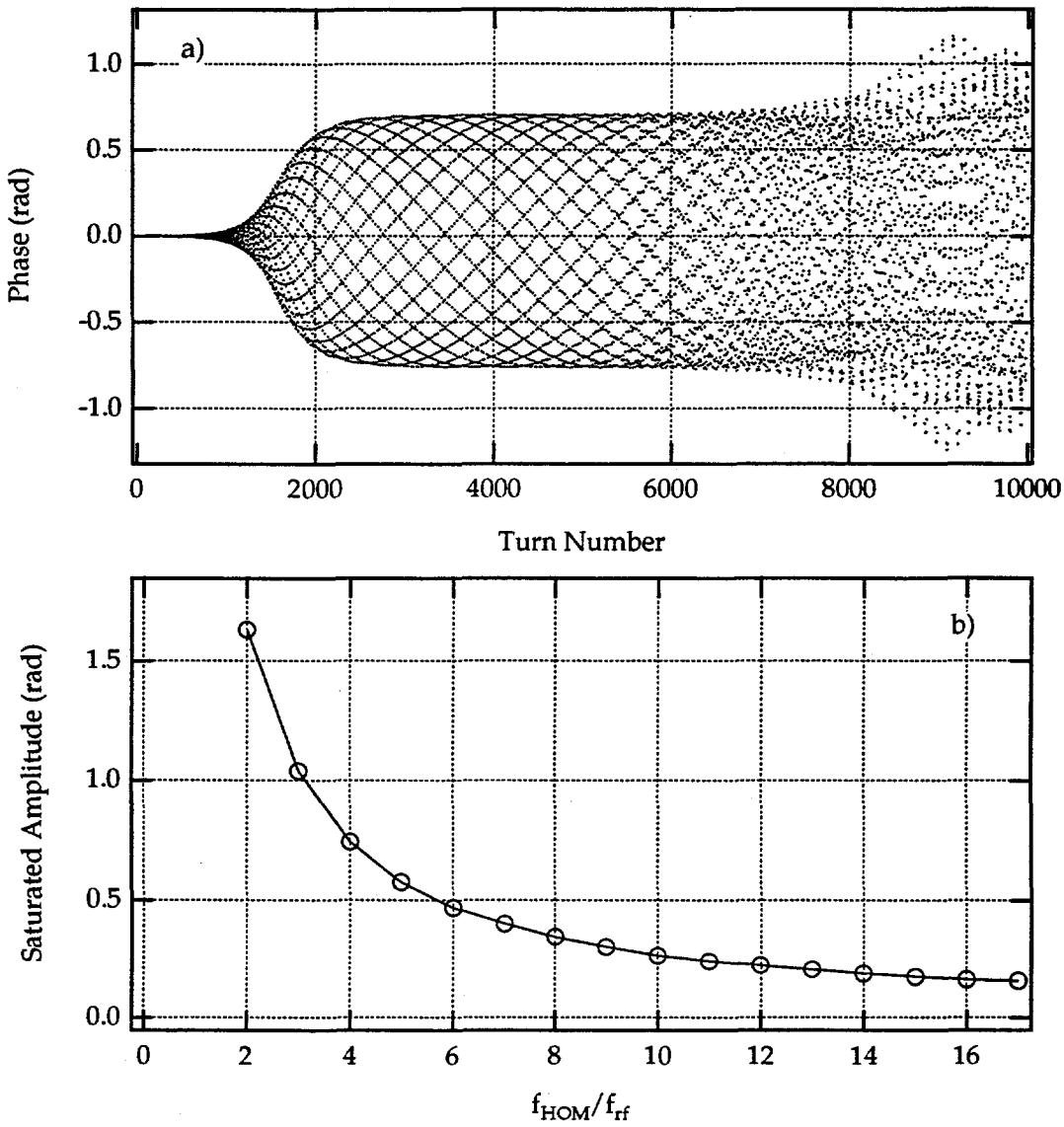


FIG. 10. Tracking simulation results. a) Saturation of growth for 4 bunches driven by a single HOM resonator at 4 times the RF frequency. Growth initially limits at $\sim \frac{\pi}{4}$. b) Saturation amplitude vs. ratio of HOM frequency to RF frequency.

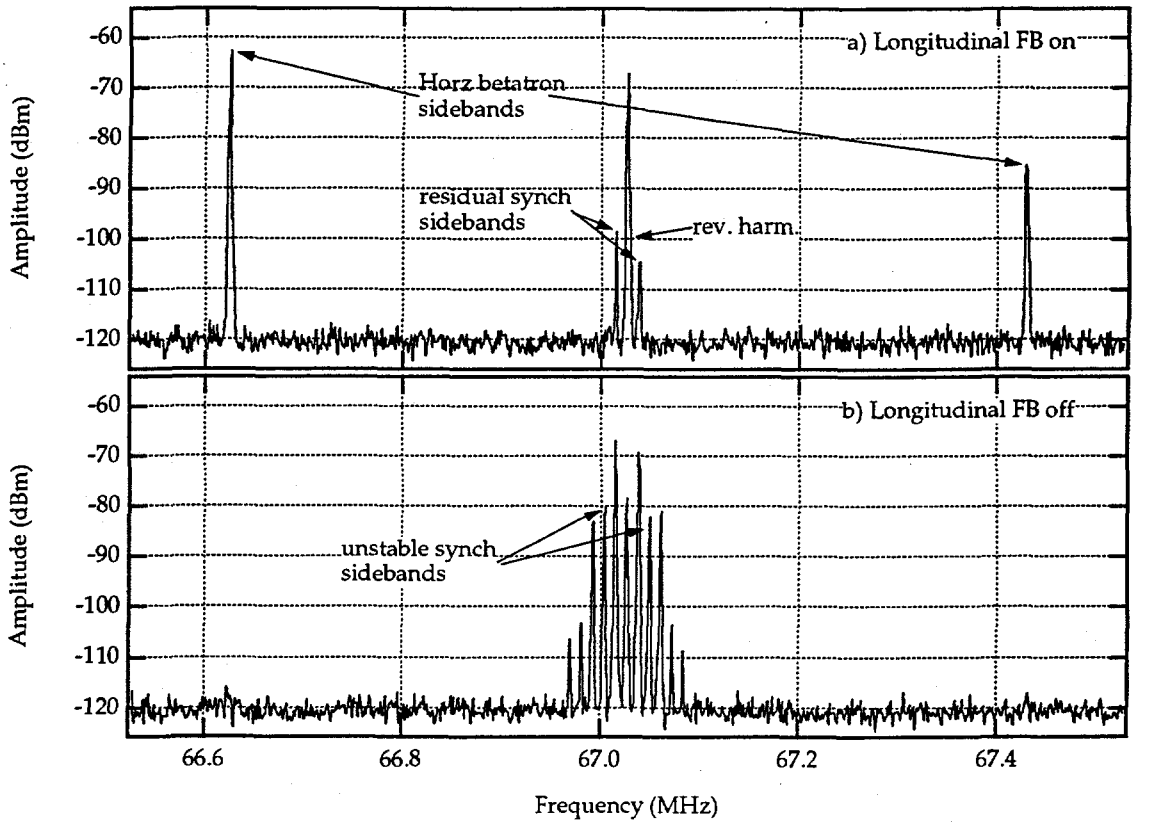


FIG. 11. Observation of the effects of longitudinal oscillations on transverse instabilities.

### B. Effects of Longitudinal Oscillations on Transverse Instabilities

As mentioned above, we were very puzzled by the observation in the ALS of strong longitudinal oscillations but very weak transverse oscillations. We have proposed two novel mechanisms to explain these observations and used computer simulations to study them. One feature of both of these mechanisms is that they do not involve any motion internal to the bunch such as head–tail or Landau damping.

The first mechanism is similar to the limiting effect of the longitudinal oscillations described above. Large longitudinal oscillations average over the transverse resonator wakefield when the amplitude of longitudinal oscillation approaches a half wavelength of the dipole wakefield, effectively averaging out the driving force. This effect is clearly seen in simulations when the transverse wakefield is a resonator–type. However, for wakefields with a relatively slow dependence on time such as the resistive wall wakefield, the phase modulation of the longitudinal oscillations has no effect.

The second limiting mechanism comes from the bunch-to-bunch betatron tune shifts generated by the large energy oscillations via the chromaticity. The tune shifts from bunch-to-bunch effectively decouple their oscillations. Because the longitudinal oscillations saturate at relatively large amplitudes, tune shifts of $\sim$0.01 can be achieved with relatively small values of chromaticity. Even for zero nominal chromaticity, the nonlinear chromaticity in the ALS is sufficient to create this effect. This effect is also observed in simulations.

The effect of the longitudinal oscillations can be tested with operation of the longitudinal feedback. Shown in Figure 11 is an example of the horizontal beam spectrum at a given revolution harmonic with and without the longitudinal feedback on. With the longitudinal feedback on, the unstable betatron sidebands are clearly evident (horizontal feedback is off.) Small noise–driven residual synchrotron sidebands are seen. When the feedback is turned off, strong unstable synchrotron sidebands appear and the horizontal sidebands disappear.

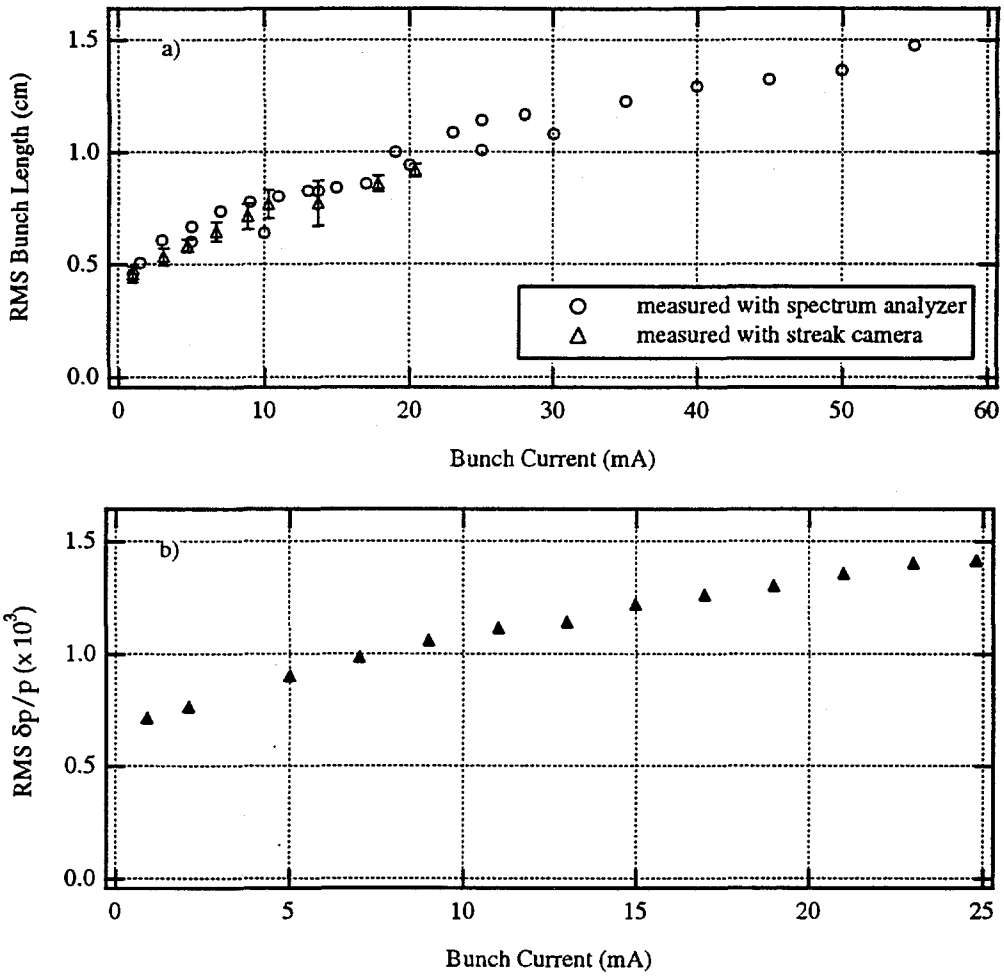


FIG. 12. a) Measured RMS bunch length vs current for $E$ =1.52 GeV and $Q_s$ =0.0075 and b) RMS energy spread vs current extracted from a transverse profile monitor.

## IV. SINGLE BUNCH MEASUREMENTS

Single bunch effects are generated by wakefields which persist over the length of bunch but generally decay before arrival of the next bunch. In the frequency domain, these wakefields are referred to as the broadband impedance. Bench impedance measurements of ALS vacuum chamber components have been conducted and are described elsewhere [5,15].

Single bunch currents up to 70 mA have been stored in the ALS, despite onset of the mode coupling instability (MCI) threshold in the vertical direction at ~28-30 mA. The vacuum chamber in one of the undulator straight sections was modified in December 1994, reducing the full height from 18 to 10 mm. Following this modification, the single bunch current was limited to ~28 mA, probably because the reduced vertical aperture no longer contained the beam at the onset of the vertical MCI. Some of the measurements presented in this section were made following the modification to the vacuum and thus are limited to a modest current range.

### A. Bunch Length and Energy Spread

Changes in the natural bunch length can typically be attributed to a combination of potential well distortion and the microwave instability (MWI). The former yields an increase or decrease in the bunch length and the latter an increase in the energy spread with a corresponding increase in the bunch length. The mea-

surements shown below indicate that bunch lengthening in the ALS is dominated by growth of the energy spread via the MWI.

We used a technique for estimating the bunch length from the broadband frequency spectrum of a single button BPM which was designed to have a broadband response. Although it is very difficult to make an absolute measurement of the bunch length or longitudinal bunch distribution using this technique because the detailed response of the pickup/cable is unknown, one can make good measurements of the relative change in bunch length assuming that the longitudinal distribution remains Gaussian and that the bunch length is known at some current. In this case, the ratio of the bunch spectra is given by

$$ratio = \frac{S_2(\omega)}{S_1(\omega)} \alpha\ e^{-\omega^2(\sigma_2^2-\sigma_1^2)} \tag{7}$$

where $S(\omega)$ is the signal as a function of frequency observed on the spectrum analyzer.

We assumed that the bunch length at low currents (<1 mA) was given by the natural bunch length and extracted the bunch length by fitting the ratio of the bunch spectra at frequencies up to ~6-7 GHz. Recent measurements with a streak camera show good agreement with the bunch spectrum technique. Results of bunch length measurements for $E$ =1.52 GeV and $Q_s$ =0.0075 are shown in Figure 12a. Fitting the data to a power law yields

$$\sigma_l(cm) = (0.36 \pm 0.03) I_b(mA)^{(0.33 \pm 0.02)} \tag{8}$$

Changes in the energy spread were extracted from measurements of the transverse beam profile at a point of dispersion in the lattice. The transverse profile is measured from synchrotron light in the UV range illuminating a BGO crystal. A video image of the profile is fit to a Gaussian. The dispersion was measured at the source point and the beta functions at the source point were extrapolated from measured values at nearby quadrupoles. The energy spread data is shown in Figure 12b. Although an increase in the energy spread vs. current is apparent, there is no clear threshold visible.

The increase in the energy spread indicates that the bunch lengthening is at least partially due to the MWI. Assuming that the bunch length changes due to potential well distortion are negligible, the bunch length above threshold as a function of current is given by

$$\sigma_l^3 = \frac{\alpha R^3}{2\pi(E/e)Q_s^2} \left| \frac{Z_\parallel}{n} \right|_{eff} I_b \tag{9}$$

The power law dependence found from the bunch length data supports the assumption that the bunch lengthening results from the MWI. From this, we calculate $|Z_\parallel/n|_{eff} = 0.22 \pm 0.07\ \Omega$. The energy spread data yields a value of $|Z_\parallel/n|_{eff} = 0.19 \pm 0.07\ \Omega$. The data from Figure 12 is shown on a log–log scale in Figure 13, along with the calculated bunch length and energy spread dependence from Eq. 9 using the above value of $|Z_\parallel/n|_{eff}$, corresponding to a threshold value of between 2.2 and 2.8 mA.

### B. Higher Order Mode Loss

We have attempted to probe the resistive part of the broadband impedance by measuring a shift in the synchronous phase angle vs. bunch current. A cavity probe signal and a BPM sum signal were compared using a vector voltmeter. The data for three natural bunch lengths in shown in Figure 14. A positive value of $\Delta\phi_s$ indicates a decrease in the synchronous phase angle (i.e. an increase in HOM loss.)

The data show the expected dependence of loss parameter on increasing bunch length. Note that the measurement at the longest natural bunch length shows an unusual increase in the synchronous phase angle. We do not yet understand the cause of this. It is difficult to interpret these measurements in terms of an effective impedance without having a model of the frequency dependence of the actual impedance. However, assuming a single broadband resonator with a resonant frequency at the average beam pipe cutoff frequency of 2.8 GHz, the measurement at the nominal natural bunch length is consistent with the broadband impedance found in the previous section.

### C. Transverse Single Bunch Measurements

The effective transverse broadband impedance is found from the measured single bunch betatron tune shift vs. bunch current and the head–tail damping rate vs. bunch current and chromaticity. We measured

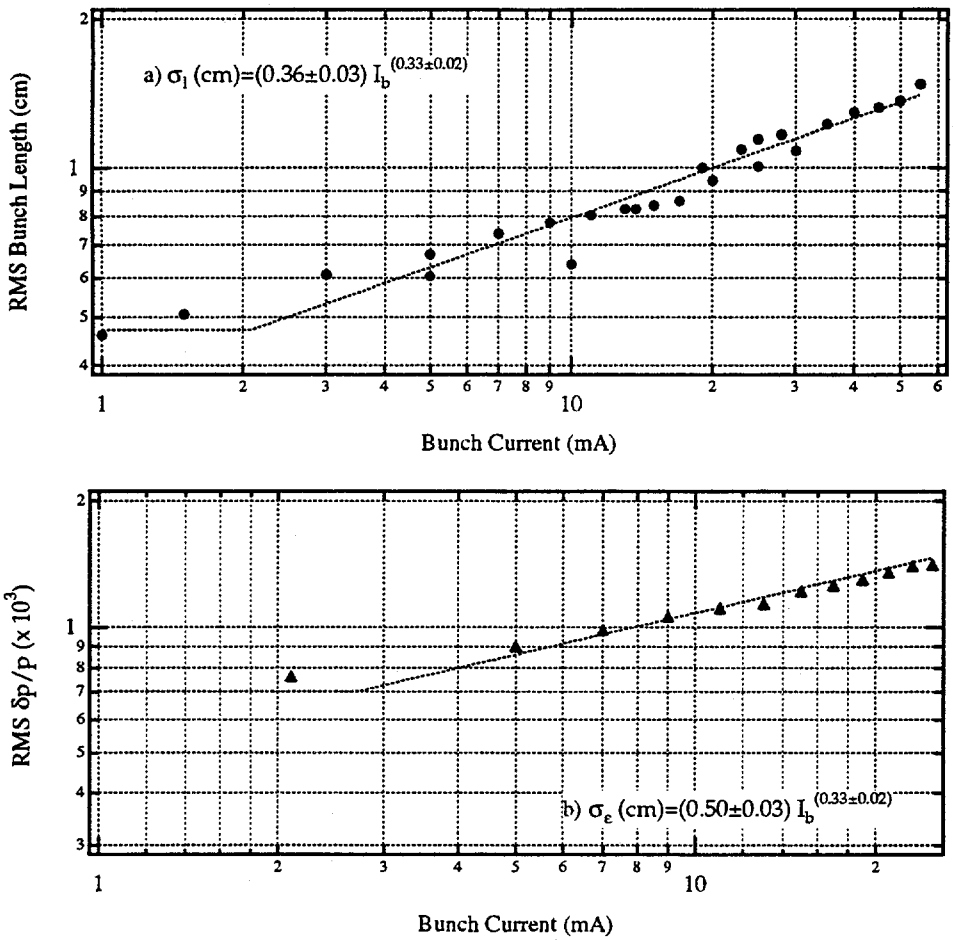


FIG. 13. a) Measured RMS bunch length vs current and b) RMS energy spread. Both data are consistent and show a 1/3 power law dependence.

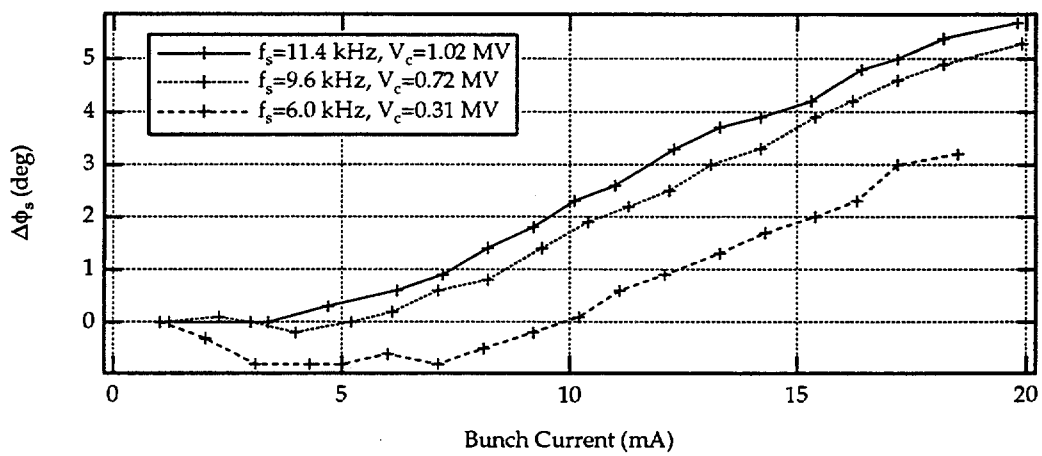


FIG. 14. Synchronous phase angle shift vs. bunch current for 3 nominal bunch lengths.

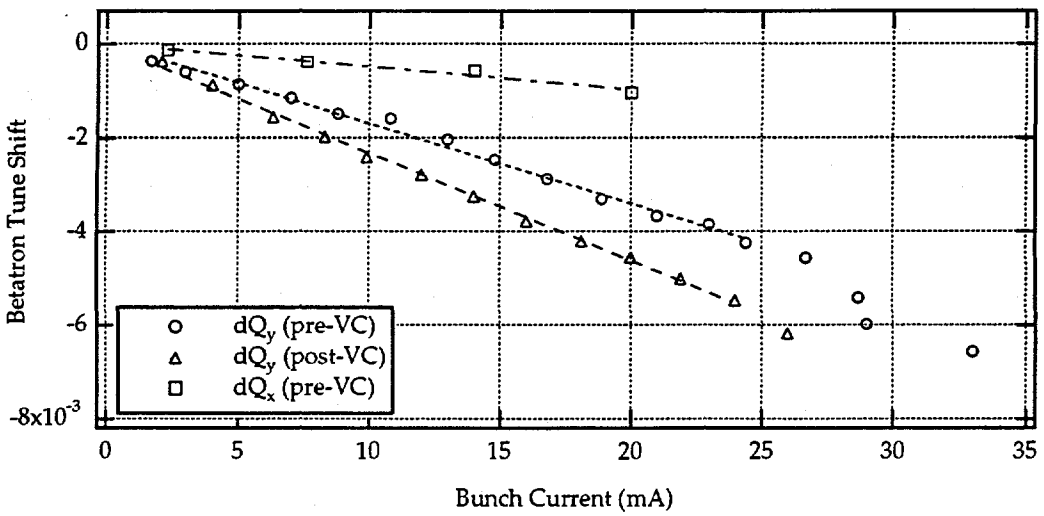


FIG. 15. Transverse tune shifts vs. current. A reduction of the vertical aperture from 18 to 10 mm in one of the straight sections resulted in a 33% increase in the effective vertical impedance.

tunes using signals from standard button BPMs with the beam driven by stripline kickers. The damping rates were measured on a spectrum analyser in tuned receiver mode using the transient from an injection bump. Unfortunately, we were not able to reliably produce measureable vertical transients. We made an effort to minimize the influence of decoherence on the damping rates by measuring the transients at the lowest possible kick amplitude.

The tune shift measurements are summarized in Figure 15. They yield values of $dQ_x/dI = -4.9 \pm 0.6 \times 10^{-5}$/mA and $dQ_y/dI = -1.71 \pm 0.05 \times 10^{-4}$/mA. Following the modification of the vacuum chamber, the vertical tune shift vs. current increased to $dQ_y/dI = -2.29 \pm 0.05 \times 10^{-4}$/mA. (Measurements before and after the modification are referred to as pre– and post–VC in Figure 15.)

The transverse tune shift of the dipole mode vs. current is related to the effective impedance by [16]

$$\frac{dQ_\perp}{dI} = \frac{R}{4\sqrt{\pi}(E/e)\sigma_l}\beta_\perp Z_{\perp,eff} \tag{10}$$

where $\beta_\perp$ is the average $\beta$–function in the lattice. We find values of $Z_{y,eff} = 155 \pm 4\ k\Omega/m$ and $Z_{x,eff} = 58 \pm 7\ k\Omega/m$. We believe the ratio of vertical to horizontal impedance results from the combination of the beampipe aspect ratio and actual relative $\beta$ functions at the locations of the impedance.

The head–tail damping rate measurements are summarized in Figure 16. They yield a value $d(\tau_x^{-1})/dId\xi_x = 1.34 \pm 0.04$/msec-mA, where the chromaticity $\xi \equiv dQ/Q/dE/E$. The range of chromaticity values corresponds to a chromatic frequency shift of $f_\xi = \xi\frac{Q_\beta}{\alpha}f_0 = 2$ GHz. A cursory check did not indicate any dependence of the damping rate on bunch length. It is difficult to interpret these measurements in terms of an effective impedance without having a model of the frequency dependence of the actual impedance. We are awaiting further measurements under a wider variety of conditions before we do this analysis.

We observe a strong steady–state blowup in the vertical beam size at 25 mA which we associate with the threshold of the mode coupling instability, which agrees well with threshold calculated from the value of the vertical impedance found from the tune shift measurements. We cannot accumulate current higher than ~28 mA. The threshold could not be increased with larger chromaticity, although very large values were not explored. The threshold is proportional to the synchrotron frequency. Prior to the change in the vacuum chamber described above, the onset of the instability occurred at ~30 mA but did not limit the beam current. The instability appears to be self-limiting, probably due to nonlinearities in the betatron motion, but at amplitudes which now exceed the vertical acceptance of the vacuum chamber. There also appears to be some hysteretic behavior in the blowup with beam current. After the onset of the instability, we must drop the current several milliamps below the threshold before it returns to its nominal size.

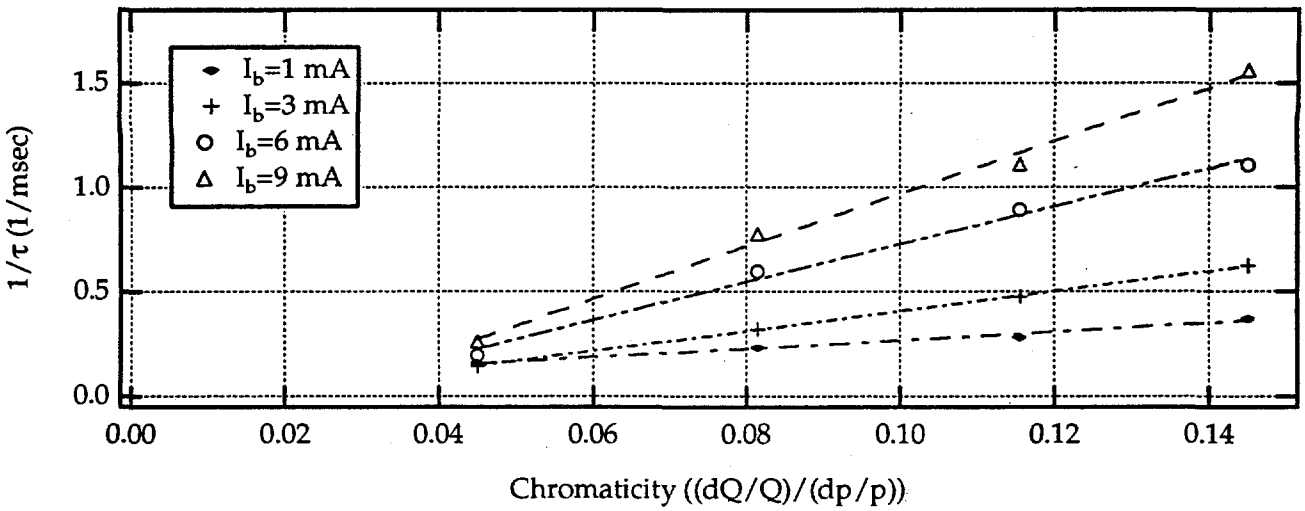


FIG. 16. Single bunch horizontal damping rates vs. chromaticity at several current levels.

## V. DISCUSSION AND CONCLUSIONS

We have presented measurements characterizing single and multibunch collective effects in the ALS. Measurments of longitudinal and transverse CB oscillations show good correlation between the unstable CB mode spectrum and the measured HOM impedance of the RF cavities. We are just beginning more detailed studies of the growth rates of all CB modes using recently commissioned feedback systems. A search for the fast ion instability showed no effect beyond the damping ability of the transverse feedback system.

Bunch length and energy spread measurements indicate the MWI as the dominant mechanism for bunch lengthening. The reduction in vacuum chamber height for decreasing gaps for insertion devices shows a measureable increase in the transverse impedance, effectively decreasing the maximum single bunch current. However, the current threshold for any significant single bunch effects is well above the typical bunch current for normal ALS operation.

## VI. ACKNOWLEDGEMENTS

We would like to thank Glen Lambertson for many useful discussions, the other members of the Center for Beam Physics, Alan Jackson, and the ALS Operations Team for support and assistance.

---

[1] J. Byrd, *Single Bunch Collective Effects in the ALS*, to appear in *Proceedings of the 1995 PAC*, May 1995.
[2] J. Byrd, J. Corlett *Measurements of Collective Effects in the ALS, Proceedings of the 1994 EPAC*, May 1994.
[3] J. Byrd, J. Corlett *Spectral characterization of longitudinal coupled–bunch instabilities at the Advanced Light Source*, to be published in *Particle Accelerators*, May 1995.
[4] J. Byrd, J. Corlett *Study of Coupled–bunch Collective Effects in the ALS, Proceedings of the 1993 PAC*, May 1993, p. 3318.
[5] J. Corlett, J. Byrd *Measurement and Computation of the Higher Order Modes of the ALS 500 MHz Accelerating Cavities, Proceedings of the 1993 PAC*, May 1993, p. 3408.
[6] R. Siemann, in *The Physics of Particle Accelerators*, AIP Conf. Proc. 184, 431 (1988).
[7] J. Leclare , *Proceedings of the 11th International Conference on High Energy Accelerators*, (Basel: Birkhauser Verlag, 1980, ed. W.S. Newman).
[8] J. Fox, et.al., in *Proceedings of the 1993 IEEE Particle Accelerator Conference*, May 1993.
[9] J. Fox, et.al., *Progress on Coupled–bunch feedback in PEP-II* in *these proceedings.*
[10] S. Krinsky, *Proceedings of the 1985 IEEE Particle Accelerator Conference*, (IEEE, New York, 1993).

[11] A. Gerasimov, Phys. Rev. E **49**, 2331 (1994).
[12] T. O. Raubenheimer and F. Zimmerman, "A Fast Beam-Ion Instability in Linear Accelerators and Storage Rings," to appear in Phys. Rev. E, SLAC–PUB–95–6740.
[13] G. Stupakov, T. O. Raubenheimer, and F. Zimmerman, "Effect of Ion Decoherence on Fast Beam-Ion Instability," submitted to Phys. Rev. E, SLAC–PUB–95–6805.
[14] S. Heifets, "Saturation of the ion–induced transverse blowup instability," PEP–II AP Note 95-20.
[15] J. N. Corlett, R. A. Rimmer *Impedance Measurements of Components for the ALS*, *Proceedings of the 1993 PAC*, May 1993.
[16] F. J. Sacherer, *Transverse Bunched Beam Instabilities–Theory*, in *Proceedings of the 9th International Conference on High Energy Accelerators*, Stanford, 1974.